JOC The Journal of Organic Chemistry

Article

pubs.acs.org/joc

10-Dimethylamino Derivatives of Benzo[*h*]quinoline and Benzo[*h*]quinazolines: Fluorescent Proton Sponge Analogues with Opposed *peri*-NMe_2/−N═ Groups. How to Distinguish between Proton Sponges and Pseudo-Proton Sponges

Alexander F. Pozharskii,*[†] Valery A. Ozeryanskii,[†] Vladimir Y. Mikshiev,[†] Alexander S. Antonov,[†] Anatoly V. Chernyshev,[‡] Anatoly V. Metelitsa,[‡] Gennady S. Borodkin,[‡] Nikita S. Fedik,[†] and Olga V. Dyablo[†]

[†]Department of Chemistry, Southern Federal University, Zorge str. 7, 344090 Rostov-on-Don, Russian Federation

[‡]Institute of Physical and Organic Chemistry, Southern Federal University, Stachki Ave. 194/2, 344090 Rostov-on-Don, Russian Federation

Supporting Information

ABSTRACT: For the first time, 10-dimethylamino derivatives of benzo[*h*]quinoline **6** and benzo[*h*]quinazoline **7a−e** as mixed analogues of archetypal 1,8-bis(dimethylamino)-naphthalene ("proton sponge") **1** and quino[7,8-*h*]quinoline **2a** have been examined. Similar to **1** and **2**, compounds **6** and **7** display rather high basicity, forming chelated monocations. At the same time, unexpected specifics of the protonated NMe_2/—N═ systems consist of a strong shift of the NH proton to the 10-NMe_2 group, contrary to the "aniline−pyridine" basicity rule. In case of **4H**$^+$, a rapid migration (in the NMR time scale) of the NH proton between two nitrogen atoms along the N−H···N hydrogen bond was registered at room temperature and frozen below −30 °C with the proton fixed on the NMe_2 group. Two different approaches for classification of strong neutral nitrogen organic bases as proton sponges (kinetically inert compounds) or pseudo-proton sponges (kinetically active) are discussed. On this basis, benzoquinoline **6** was identified as staying closer to pseudo-proton sponges while **7a−e** to proton sponges due to the presence in their molecules of bulky substituents in the pyrimidine ring. Other remarkable peculiarities of **6** and **7** are their yellow color and luminescence in the visible region distinguishing them from colorless **1** and **2a**.

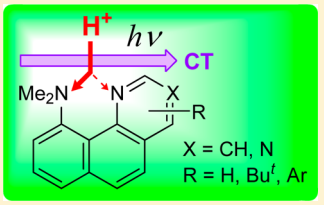

INTRODUCTION

It is generally recognized that the abnormally high basicity (pK_a = 12.1, H_2O; 7.5, DMSO; 18.5, MeCN, 25 °C) of 1,8-bis(dimethylamino)naphthalene (**1** or DMAN), also known under the "Proton-sponge" trademark, ultimately stems from the electrostatic repulsion of the juxtaposed unshared nitrogen electron pairs, which strongly destabilize the base.[1] Such repulsion is canceled at the formation of chelated monocation **1H**$^+$ resulting in considerable free energy gain. For decades, this structural motif stimulated designing many other neutral superbases possessing even stronger basicities than **1** (see Schemes 1 and 2 and refs 1a and 2). As a classic example, the investigation of quino[7,8-*h*]quinoline **2a** by Staab and his co-workers[3] can be mentioned. They reasoned that a more strict mutual orientation of the free electron pairs of two aza-groups in **2a** might strengthen the electrostatic repulsion thereby increasing basicity. This expectation had been in part justified: the pK_a of **2a** equal to 12.8 (H_2O) turned out to be 0.7 logarithmic units larger compared with that of **1**. Another important difference between molecules **1** and **2a** was connected with rates of their protonation−deprotonation. While the protonation of **2a**, as in cases of ammonia and other common bases, occurs practically with the diffusion rate (~10^{10} L mol^{-1} s^{-1}), the rate of addition-elimination of a proton for DMAN is about 5 orders of magnitude lower.[4] Thus, the combination of both factors, high thermodynamic basicity and relatively low kinetic activity, actually determines the "proton sponge" phenomenon.[1,2] On this basis, **2a** should be more correctly classified as a compound structurally related to

Scheme 1. 1,8-Bis(dimethylamino)naphthalene (1) and Quino[7,8-*h*]quinoline (2a) as Archetypal Representatives of Proton Sponges and Pseudo-Proton Sponges

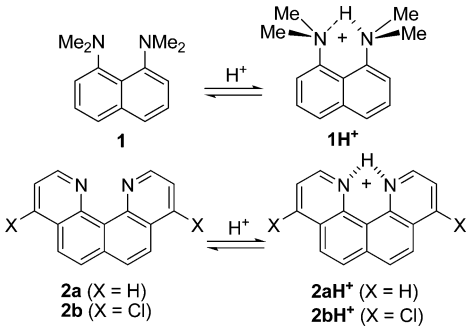

Received: April 22, 2016
Published: June 10, 2016

DOI: 10.1021/acs.joc.6b00917
J. Org. Chem. 2016, 81, 5574−5587

Scheme 2. Previously Known Representatives of the *peri*-NMe_2/—N═ Systems

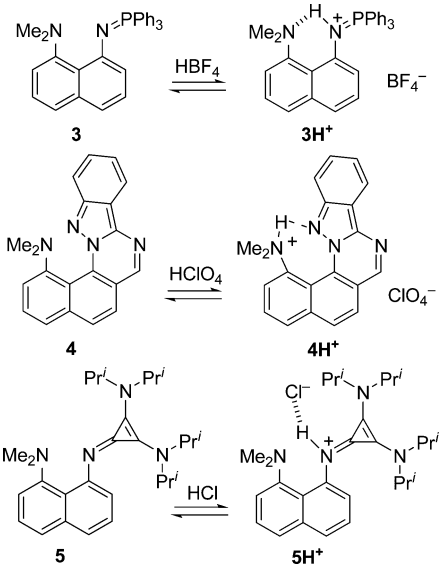

Scheme 3. NMe_2/—N═ Systems Studied in This Work

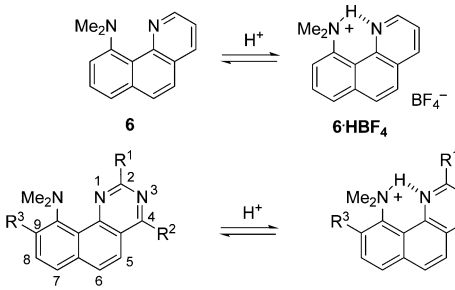

proton sponges or as a proton sponge-like compound or, shorter, as a pseudo-proton sponge.[2,5] One more peculiarity of **2a** is the ease of addition of other Lewis acids, for example, heavy metal ions.[6] In contrast, DMAN normally displays inertness (low nitrogen nucleophilicity) to the Lewis acids bulkier than a proton except a few cases, mostly including boron-containing spieces.[7]

In this light, it seemed rather intriguing to study the mixed analogues of compounds **1** and **2a** with the NMe_2 and aza groups opposed to each other in the *peri*-positions. As far as we know, to date there have been reported only three examples of such the NMe_2/—N═ "hybrid" bases (Scheme 2), namely, 1-dimethylamino-8-triphenylphosphoranylideneaminonaphthalene (**3**),[8a,b] *N,N*-dimethylbenzo[*h*]indazolo[2,3-*a*]quinazoline-1-amine (**4**),[8c] and 1-dimethylamino-8- [bis(diisopropylamino)cyclopropenylideneimino]naphthalene (**5**).[8d] Compounds **3** and **4** are similar in that in the solid they both form the chelated protonated forms **3H**$^+$ and **4H**$^+$, while for **5·HCl**, X-ray study has revealed an absence of any intramolecular hydrogen bonding (IHB) but instead a hydrogen bond between the NH proton and the chloride counteranion. From this, it follows that **5** can be ascribed to the pseudo-proton sponges and its high basicity (pK_a 23.8, MeCN) almost entirely originates from that of the bis(diisopropylamino)cyclopropenimine residue itself (pK_a 27.0, MeCN, calculated value).[9]

In the present article, we report on the properties of the previously unexplored NMe_2/—N═ azine superbases involving their simplest representative, 10-dimethylaminobenzo[*h*]quinoline (**6**), and several derivatives of 10-dimethylaminobenzo[*h*]quinazoline (**7a**—**e**) (Scheme 3). As an exception, the indazole-based system **4** was also examined somewhat deeper than before. We focus mainly on their structure, basicity, and some spectral and electronic characteristics.

RESULTS AND DISCUSSION

Preparation. 10-Dimethylaminobenzo[*h*]quinoline **6** was obtained as brown-orange oil in 6% yield by Skraup cyclization of 1-dimethylamino-8-aminonaphthalene,[10] and its structure was confirmed by spectral measurements (Figures S1 and S2, Supporting Information). Synthesis of benzo[*h*]quinazolines **7a**—**e** has been performed via rather interesting chemistry and is published separately.[11] On treatment with tetrafluoroboric acid, compound **6** produces salt **6·HBF$_4$**, isolated as light-beige needles. Tetrafluoroborates and perchlorates of quinazolines **7a**—**e** were prepared similarly.

Properties of IHB in the Protonated Forms. As it is seen from the ^{1}H NMR spectra (Figures S3—S14, Supporting Information) in all protonated salts obtained, the NH proton appears as a low field broadened peak at δ 16—19 ppm, which is typical for proton sponge cations and indicates the formation of an IHB (Table 1). Even so, on the whole the NH proton in cations **6H**$^+$ and **7H**$^+$ resonates at higher frequencies compared with that of DMAN and quino[7,8-*h*]quinoline salts. Thus, for salt **6·HBF$_4$** in CD_3CN and DMSO-d_6 δ_{NH} = 17.5 and 16.8 ppm, respectively, and for quinazoline cations **7a—d·H**$^+$, this value is even smaller (δ_{NH} = 15.9—17.3 ppm). The only exception (δ_{NH} = 19.1 ppm, CD_3CN) is tetrafluoroborate **7e·HBF$_4$**, which most likely originates from the so-called "buttressing effect" exhibiting by the 9-bromine atom with regard to the 10-NMe_2 group (for close examples of such phenomenon, see ref 13).

The second peculiarity of the solution structure of cations **6H**$^+$ and **7H**$^+$ is a strong asymmetry of their NHN hydrogen bridges. As a measure of such asymmetry, the "proton localization" index, PL, was suggested earlier.[14a] It is based on the observation that when a proton is entirely located on the aniline NMe_2 group, as in case of *N,N*-dimethylanilinium cation,[15] the spin—spin coupling constant $^3J_{NH,NMe}$ is normally about 5.2 Hz. In the usually symmetric cation **1H**$^+$, the NH proton in the NMR time scale equally belongs to two nitrogen atoms, and the value $^3J_{NH,NMe}$ is halved to ~2.6 Hz, remaining 5.2 Hz totally. For asymmetric derivatives of DMAN, both $^3J_{NH,NMe}$ constants become different but their sum still remains near 5.2 Hz, from which it is easy to calculate the PL. Of course, such calculations may seem rough, but other estimates of the PL, in particular based on the differences between the coupling constants of the NH proton with two ^{15}N nitrogen atoms, give quite close results.[14b—d]

As depicted in Table 1, the NH proton in cation **6H**$^+$ in both CD_3CN and DMSO-d_6 by 90% resides on the NMe_2 group ($^3J_{NH,NMe}$ = 4.7 Hz). In most benzoquinazoline cations **7H**$^+$, the hydrogen bond asymmetry is even larger reaching in some cases 96% (a small deviation of salt **7e·HBF$_4$** with PL = 87/13 can be again assigned to the buttressing effect). It is worth noticing that such strong shift of the NH proton to the NMe_2 group in **6H**$^+$ and **7H**$^+$ is rather unexpected. Indeed, among the

DOI: 10.1021/acs.joc.6b00917
J. Org. Chem. 2016, 81, 5574—5587

Table 1. Chemical Shifts, δ_{NH}, of Chelated NH Proton, Proton Localization Indices, PL, and Selected Parameters of Hydrogen Bridge in Cations of Mixed NMe_2/—N═ Systems

	δ_{NH}, ppm ($^3J_{NH,NMe}$, Hz)		IHB parameters (X-ray data); bond lengths and distances (Å), angles (deg)				
structure and references	CD_3CN	DMSO-d_6	N···N	N−H	H···N	∠NHN	PL,[a] %
1·HBF$_4$[12]	18.69 (2.6)	18.33 (2.6)	2.564	1.30	1.31	159	50/50 (MeCN)
							50/50 (DMSO)
							50/50 (X-ray)
2b·HBF$_4$[6b]		19.29	2.591	0.86	1.90	136	69/31 (X-ray)
3·HBr[8a,b]		18.43	2.519	1.20	1.38	155	46/54 (X-ray)
4·HClO$_4$[8c]	18.15 (4.20)[b]		2.550	0.96	1.61	170	81/19 (MeCN)[b]
							63/37 (X-ray)
6·HBF$_4$[c]	17.53 (4.7)	16.80 (4.7)	2.620	0.96	1.75	148	90/10 (MeCN)
							90/10 (DMSO)
							65/35 (X-ray)
7a·HBF$_4$[c]	16.88 (4.9)	15.93 (4.7)					94/6 (MeCN)
							90/10 (DMSO)
7a·HClO$_4$[c]	16.84 (5.0)	15.91 (4.5)	2.631[d]	1.04[d]	1.77[d]	137[d]	96/4 (MeCN)
			2.613[d]	1.11[d]	1.64[d]	142[d]	87/13 (DMSO)
							63/37 (X-ray)[d]
							60/40 (X-ray)[d]
7b·HBF$_4$[c]	17.21 (4.8)	16.28 (4.5)					93/7 (MeCN)
							87/13 (DMSO)
7c·HBF$_4$[c]	16.45 (2.88)						55/45 (MeCN)
7d·HBF$_4$[c]	17.29 (4.9)	16.28 (4.7)					94/6 (MeCN)
							90/10 (DMSO)
7e·HClO$_4$[c]	19.14 (4.5)		2.569	1.02	1.61	156	87/13 (MeCN)
							61/39 (X-ray)

[a]For asymmetric cations **3H$^+$**, **4H$^+$**, **6H$^+$**, and **7H$^+$**, the first value in the fraction refers to the NMe_2 group. PL values from X-ray measurements were calculated as a ratio of N−H or N···H lengths to their sum. [b]At−45 °C; other ^{1}H NMR data were obtained at 25 °C. [c]This work. [d]For two independent molecules.

nitrogen derivatives of arenes, an apparently yet clearly undeclared rule exists that monoazaarenes are always somewhat more basic than their structurally related aniline analogues: pyridine (pK_a = 5.25) > *N*,*N*-dimethylaniline (pK_a = 5.12), quinoline (pK_a = 4.87) > 1-dimethylaminonaphthalene (pK_a = 4.43), benzo[*h*]quinoline (pK_a = 4.25) > 4-dimethylaminophenanthrene ($pK_a \approx 4.0$) (Figure S31, Supporting Information). Surprisingly, this rule is valid even for a pair of superbasic compounds, **1** and **2a**. We find it difficult to clearly explain the violation of the "aniline−pyridine" basicity rule for **6**. Possibly, this is caused by some peculiarities of the IHB in cation **6H$^+$**, for example, larger energy gain for Me_2N^+−H···N═ hydrogen bonding in comparison with Me_2N···H−N^+═. In the case of benzoquinazolines **7**, the tendency of the proton to be shifted toward the NMe_2 group is obviously strengthened by their low aza basicities (see below).[16] The situation considerably changes in the 2,4-dithienyl derivative **7c** whose cation contains the NH-proton placed almost symmetrically although still closer to the NMe_2 group (PL = 55/45 in CD_3CN). This can be attributed to the enhanced ability of the 2-thienyl group to stabilize positively charged centers (σ^+ = −0.43).[17]

A special and very interesting case is cation **4H$^+$**. Previously,[8c] we have demonstrated the existence of a short IHB (N···N 2.55 Å) in the solid salt **4·HClO$_4$**, wherein, similarly to cations **6H$^+$** and **7H$^+$**, the bridge proton in **4H$^+$** is shifted to the NMe_2 group though less strongly (Table 1). Judging by value of the chemical shift (δ_{NH} = 18.15 ppm, CD_3CN), the IHB in **4H$^+$** under ambient conditions persists also in solution but surprisingly without any coupling of the NH proton to the NMe_2 group. There can be two reasonable explanations of this fact: (1) the NH proton in **4H$^+$** in solution almost completely passes to the aza group or (2) the bridge proton equilibrates rapidly on the NMR time scale between both nitrogen atoms. To choose between these two possibilities in the present work, we have conducted temperature dependent ^{1}H NMR measurements for **4·HClO$_4$** in CD_3CN solution (Figure 1). It turned out that already at −40 °C the primarily sharp singlet of the NMe_2 group splits into a nicely resolved doublet with $^3J_{NH,NMe}$ = 4.0 Hz (PL = 77%) and at −45 °C the coupling increases to 4.2 Hz bringing the PL on the NMe_2 group to 81%. Simultaneously, the NH signal on decreasing the temperature appears as a broaden septet and moves to higher field: 18.15 ppm at 25 °C and 17.83 at −45 °C.[18] In our opinion, this experiment unambiguously confirms that the IHB in **4·HClO$_4$** differs by high mobility, and therefore the second explanation is correct. The quantum-chemical calculations (B3LYP/6-311++G**, acetonitrile) have revealed that the energy difference between tautomers **4H$^+$**(a) and **4H$^+$**(b) in MeCN is of 1.9 kcal mol^{-1} in a favor of the former and the barrier for conversion **4H$^+$**(a) → **4H$^+$**(b) is about 2.1 kcal mol^{-1} (Figure 2). The driving force for this phenomenon seems to consist in preserving aromaticity of the indazolium and pyrimidinium heterocyclic moieties on transition to **4H$^+$**(b), which somehow balances larger stability of form **4H$^+$**(a). Possibly, the enhanced linearity of the NHN hydrogen bonding in **4H$^+$** (Table 1) also contributes to the low energetic barrier. Anyway, cation **4H$^+$** can be viewed as an instructive model of the proton-transfer enzymes, for example, chymotrypsin.[19] For comparison, we have estimated the energy of similar proton transfer in benzoquinazolinium cation **7aH$^+$**. As

DOI: 10.1021/acs.joc.6b00917
J. Org. Chem. 2016, 81, 5574−5587

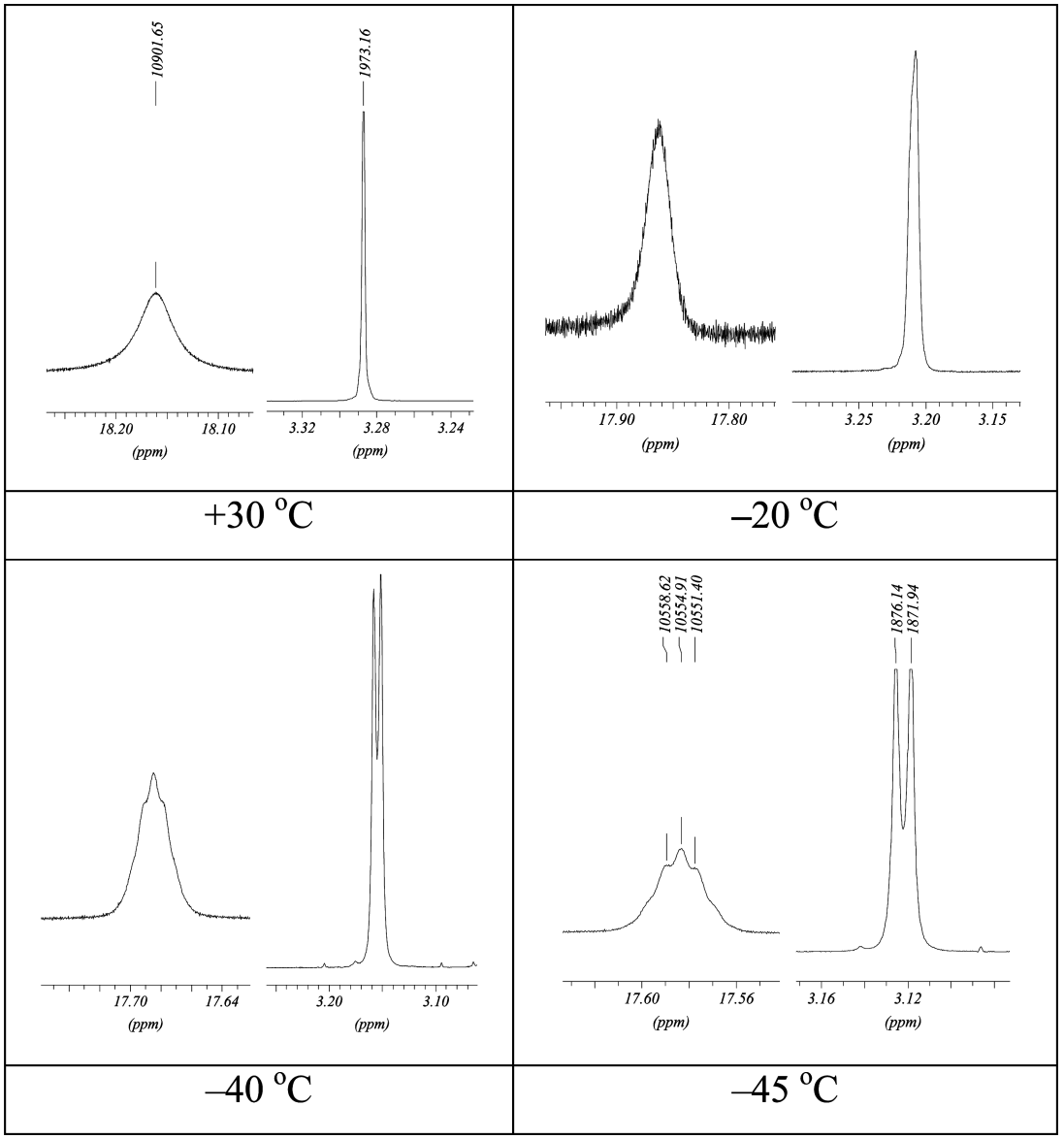

Figure 1. Chelated NH proton and NMe_2 region plots of the ^1H NMR spectra recorded for perchlorate **4·HClO$_4$** at different temperatures (MeCN, 600 MHz).

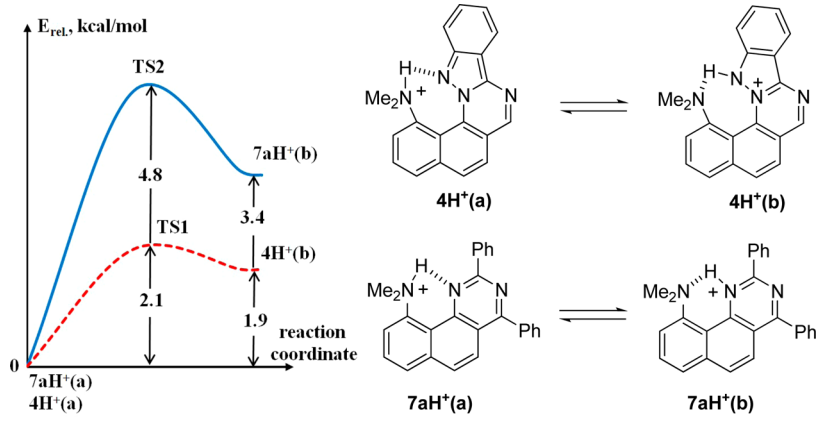

Figure 2. Theoretically calculated (B3LYP/6-311++G**, acetonitrile) potential energy curves for proton transfer in cations **4H$^+$** and **7aH$^+$** (in MeCN); the total energies of forms **4H$^+$**(a) and **7aH$^+$**(a) were chosen as reference ones (E_{rel} = 0.0 kcal mol^{-1}).

seen from Figure 2, the barrier to transition **7aH$^+$**(a) → **7aH$^+$**(b) turned out to be 2-fold higher than that for **4H$^+$**. Not surprisingly, the splitting of NMe_2 group on the NH proton in the ^1H NMR spectrum of **7aH$^+$** in CD_3CN is still observed

DOI: 10.1021/acs.joc.6b00917
J. Org. Chem. 2016, 81, 5574–5587

even at 76 °C although the $^3J_{NH,NMe}$ value decreases from 4.92 to 4.37 Hz (Figures S24 and S25, Supporting Information).

Basicity and Kinetic Activity. Next, we measured the pK_a values of **6** and **7** in CD_3CN and DMSO-d_6 by the competitive method using NMR monitoring.[3] The transprotonation experiments with proton sponge **1** and its 2,7-dibromide **8** as the reference compounds for monoprotonated bases **6** and **7**, respectively, were conveniently performed to give the data depicted in Table 2 and in Figures S26 and S27. It has been found that **6** with pK_a = 7.7 (DMSO-d_6) or 12.3 (in H_2O scale) exhibits 0.2pK_a units higher basicity than DMAN but is less basic than quino[7,8-*h*]quinoline **2a**. The basicity of benzo[*h*]-quinazolines **7a–d** ranges between pK_a = 5.3 and 5.9 in DMSO-d_6 and 16.0 and 16.6 in CD_3CN. The lower pK_a values for **7** result from generally small basicity of quinazolines owing to the presence of two electron-accepting aza groups (for example, pK_a of 4-methylquinazoline in water is 2.52).[20] Nevertheless, to our knowledge, compounds **7** are the most basic quinazolines known to date.

Table 2. Basicity Values, pK_a (25 °C), of Proton Sponge 1 and Some of Its Monoaza- and Diaza-*peri*-Analogues[a]

	solvent			solvent	
compd	MeCN	DMSO	compd	MeCN	DMSO
1	18.5	7.5	**7a**	16.0	5.3
2a		8.2	**7b**	16.4	5.5
5	23.8		**7c**	16.2	5.5
6		7.7	**7d**	16.6	5.9

[a]Attempts to measure pK_a values of **3** and **7e** failed due to hydrolytic instability of the base in the first case[8b] and bad solubility in the second.

It is noteworthy that in the ^{1}H NMR spectrum of the mixture shown in Figure S26, most peaks belonging to cation **6H$^+$** are considerably broadened relatively those of **1H$^+$**. Apparently, this reflects kinetic activity of **6** (at least in the NMR time scale) and thus questions its proton sponge nature. This opinion is strengthened when considering the X-ray structure of **6·HBF$_4$** resolved in this work (Figure 3b). Due to the absence of one NMe_2 group in **6**, the hydrophobic pocket between the *peri*-substituents here is not as narrow as in salts of the original proton sponge, for example, **1·HBF$_4$** (Figure 3a). This explains why the distance between the NH proton and the BF_4^- anion in **6·HBF$_4$** is much less (2.49 Å) than that in **1·HBF$_4$** (2.91 Å).

Properties similar to **6·HBF$_4$** might be also expected for salts of the parent 10-dimethylaminobenzo[*h*]quinazoline (**7**, R^1,R^2,R^3 = H), but unfortunately this compound is not available. For its derivatives **7a–e**, their kinetic activity seems to be inhibited by the presence of the aryl or hetaryl substituent in position 2. Such view follows from the large distance (3.74 and 3.88 Å for two independent molecules) between the perchlorate anion and the NH proton in the solid salt **7a·HClO$_4$**, which excludes any perceptible interaction between them (Figure 3c,d). The NH–anion distance is even larger (4.08 Å) in **7e·HClO$_4$** due to flattening of the 10-NMe_2 group that results in narrowing the internitrogen pocket (Figure 3e). Thus, the sums of the CNC valence angles at the NMe_2 group, $\sum$N, in **7eH$^+$** and **7aH$^+$** are equal to 342° and 336°, respectively.

Structural Criterion for Classification of Neutral Organic Superbases. Based on the foregoing considerations, we thought that the X-ray NH···anion distances could be used for rather clear classification of neutral superbases either as proton sponges or pseudo-proton sponges.[21,22] Normally, a counterion tends to get closer to the NH proton. In proton sponges, this process is considerably hindered by the tightness of the hydrophobic pocket. Therefore, the NH···counteranion distance for proton sponges should be substantially larger than that for kinetically active bases. One can imagine that for each type of solid salts under strictly predetermined conditions, such as an arbitrarily chosen anion[22] and temperature, there should exist a characteristic NH···anion distance allowing reasonable classification. Regrettably, there is not much systematic information on the subject. Nevertheless, some available data including those obtained in this work are collected in Table 3.

Table 3. X-ray Anion–Cation Interaction-based Classification of Proton Sponges and Related Compounds

cation	counterion, X^-	*T*, K	X···H[a] (Å)	classification of base	ref
1H$^+$	BF_4^-	295	2.91	proton sponge	12
1H$^+$	Br^-	295	3.69	proton sponge	24
1H$^+$	F^-	295	2.76[b]	proton sponge	25
2bH$^+$	BF_4^-	173	2.09	pseudo-proton sponge	6b
2cH$^+$	BF_4^-	100	3.37	proton sponge	23e
3H$^+$	Br^-	295	4.49	proton sponge	8a
3H$^+$	BF_4^-	295	3.36	proton sponge	8a
3H$^+$	PF_6^-	295	4.44	proton sponge	8a
4H$^+$	ClO_4^-	120	3.45[c]	proton sponge	8c
5H$^+$	Cl^-	295	2.29[d]	pseudo-proton sponge	8d
6H$^+$	BF_4^-	120	2.46	pseudo-proton sponge	this work
7aH$^+$	ClO_4^-	120	3.74; 3.88[e]	proton sponge	this work
7eH$^+$	ClO_4^-	120	4.08[c]	proton sponge	this work
9H$^+$	BF_4^-	173	2.05[d]	pseudo-proton sponge	26
10H$^+$	ClO_4^-	295	2.32[d]	pseudo-proton sponge	27

[a]Distance between the NH proton and the nearest atom X of the counteranion. [b]The shortest anion–cation distance known to date for the proton sponge salts. [c]Absence of visible anion–cation interaction; the anion is situated side-away from the cation due to spatial hindrance exerted by aryl or ester substituents. [d]Absence of proton chelation. [e]For two independent molecules.

One can see that for DMAN cation **1H$^+$**, the shortest distances between the NH proton and a counterion are those for F^- and BF_4^- (2.75 and 2.91 Å, respectively). This means that all bases for which these values are nearly the same or larger can be considered as proton sponges. In contrast, superbases with lesser NH···anion distances should be classified as pseudo-proton sponges. Thus, five of 11 chosen compounds, namely, **2b**, **5**, **6**, 2,2′-bipyridinium tetrafluoroborate **9**, and 1,10-phenanthrolinium perchlorate **10** fall into the last category. Remarkably, unlike **2b**, its counterpart **2c** obviously belongs to proton sponges due to the steric shielding of the internitrogen space by two ethoxycarbonyl groups (Scheme 4).

One of the advantages of the solid state-based classification of superbases stems from the considerable dependence of their kinetic activity on solvent properties (for influence of solvent on dynamics of the proton transfer and the NH···anion interaction in protic salts of **1**, see ref 22). For example, in the

DOI: 10.1021/acs.joc.6b00917
J. Org. Chem. 2016, 81, 5574–5587

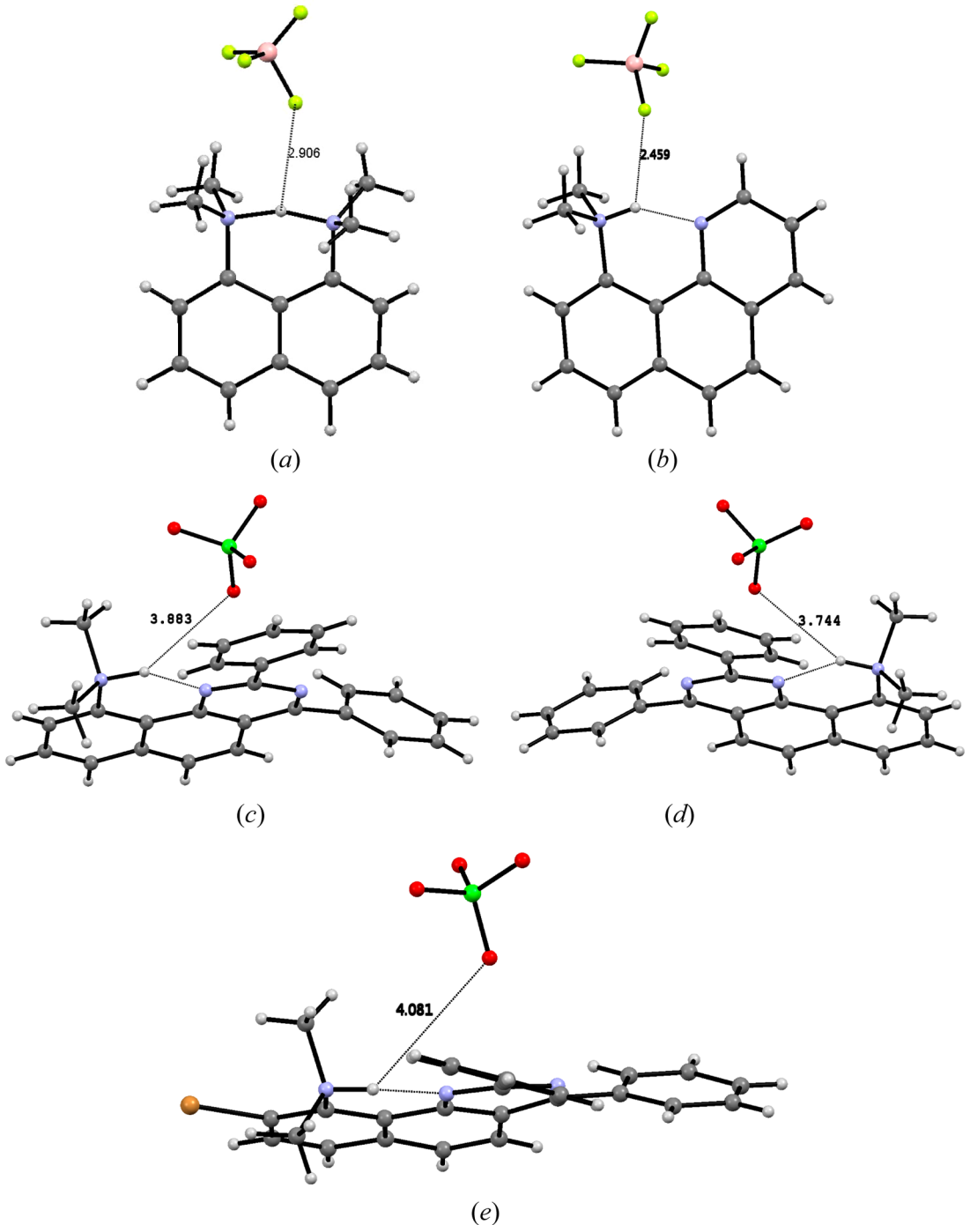

Figure 3. Molecular structures of some salts showing different modes of interaction (Å) between the NH proton and counteranion: (a) **1**·HBF_4; (b) **6**·HBF_4; (c,d) two independent molecules of **7a**·$HClO_4$; (e) **7e**·$HClO_4$.

^{1}H NMR spectrum of equilibrating **7bH**$^+$ and **7b** forms in MeCN, the NMe_2 groups are indistinguishable in the NMR time scale and give a single broaden peak at 3.11 ppm (non-proton sponge behavior). In contrast, the same mixture in DMSO-d_6 exhibits separate peaks for these groups at 3.01 and 3.68 ppm indicating low kinetic activity and the proton sponge status of **7b** (Figure 4, see also Figures S28−S30, Supporting Information).

The kinetic activity is also sensitive to temperature changes. Thus, in the ^{1}H NMR spectrum of a 1:1 mixture of **7a** and **7a**·HBF_4 at 20 °C, merging of the NMe_2 peaks of both species is observed while at −20 to −40 °C, their signals are separated suggesting pseudo-proton sponge and proton sponge behavior, respectively. At the same time, as we have demonstrated here for the first time, DMAN displays proton sponge properties not only in different media (CD_3CN and DMSO-d_6 were tested) but even at elevated temperature (up to 170 °C in DMSO-d_6) (Figures S21−S23, Supporting Information).

UV−Vis Spectra and Participation of Basic Centers in Conjugation. Working with compounds **6** and **7**, we drew attention to another peculiarity: unlike colorless **1** and **2a**, they are yellow in color and display fluorescence in the visible region. The obvious reason for this is a direct conjugation of the dimethylamino and aza groups through the naphthalene π-

DOI: 10.1021/acs.joc.6b00917
J. Org. Chem. 2016, 81, 5574−5587

Scheme 4. Some Auxiliary Compounds Mentioned in the Article

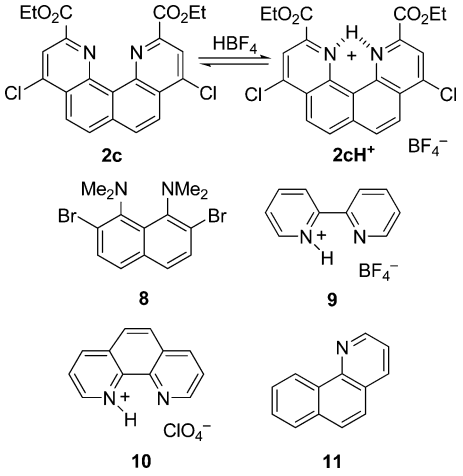

Scheme 5. Conjugation of *peri*-Substituents in Compounds 6 and 7

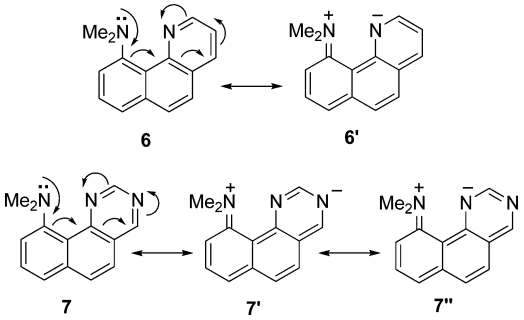

system, which can be represented by the mesomeric (**6** and **7**) or resonance structures (**6** ↔ **6′** and **7** ↔ **7′** ↔ **7″**) shown in Scheme 5.

Commonly, such conjugation between strong electron-donating and electron-accepting groups considerably diminishes the energy difference between the highest occupied (HOMO) and the lowest unoccupied (LUMO) molecular orbitals and causes bathochromic shift of the long wavelength band in the electron absorption spectrum. Figures 5 and 6, as well as Table 4, demonstrate that this is indeed the case. Thus, unlike proton sponge **1** (λ_{max} = 341 nm), a very diffuse long wavelength band of compound **6** is centered at 390 nm with the end absorption tailing up to 430 nm. In the UV−vis spectrum of its quinazoline analogue **7a**, the maximum of the more resolved long wavelength band lies at 420 nm and the end absorption spreads into the 470 nm region. The conjugation could be more effective at higher coplanarity of the 10-NMe_2 groups and the naphthalene system but in accordance with the X-ray measurements[11] the rotation angle, ϕ, for the NMe_2 group plane relative to the mean ring plane in **7a** is 44.6° (ϕ = 59.8° in **7e** and 40° in **1**). One can calculate, using the well-known[28] ratio $M = M_0 \cos^2 \phi$, that the remaining conjugation in **7a** (M) is 50% of that (M_0) in an ideally flat and coplanar model. Apparently, such large value of ϕ in **7a** and very likely in **6** is caused not so much by steric reasons (this is not spread on **7e**) as electrostatic repulsion between the free electron pairs of the *peri*-substituents.

We also believe that the first excited electronic state for molecules **6** and **7** closely corresponds to zwitterionic resonance structures of type **6′**, **7′** ,and **7″** as indicated by frontier orbital images (Figure 7). As seen, the electron transfer from HOMO to LUMO in **6** and **7** occurs from the 10-NMe_2 group toward the azine ring. Unlike **6** and **7**, in proton sponge **1** and quino[7,8-*h*]quinoline **2a**, the charge transfer on excitation takes place from the NMe_2 groups into the naphthalene system or from the latter to the aza groups.

Generally, a direction of the electronic displacement in the excited and ground states of molecules **1**, **2a** ,and **7** is about the same as one that can be expressed in a visual form via the total vector of the dipole moment, characterizing a distribution of

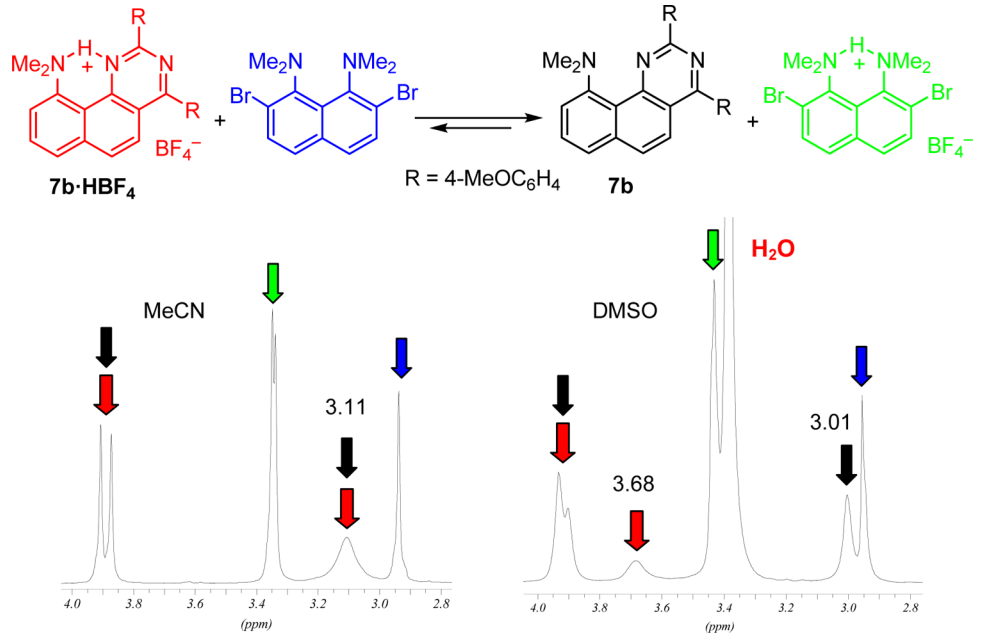

Figure 4. ^{1}H NMR aliphatic region plots of the equimolar equilibrating mixtures of salt **7b·HBF$_4$** and dibromonaphthalene **8** showing solvent influence on the kinetic behavior of **7** (250 MHz, 20 °C; color code as in the scheme above).

DOI: 10.1021/acs.joc.6b00917
J. Org. Chem. 2016, 81, 5574−5587

Table 4. Position of Long-Wavelength Band in UV−Vis Spectra of Proton Sponge 1 and Some of Its Analogues in $CHCl_3$ and Calculated Energies of Frontier Orbitals for Gas Phase and Chloroform Solution (in Brackets) (B3LYP/6-311++G)**

			orbital energies, E, eV		
compound	λ_{max}, nm ($CHCl_3$)	ε	HOMO	LUMO	$E_{HOMO} - E_{LUMO}$
1	341	11690	−5.190 (−5.250)	−1.061 (−1.161)	4.129 (4.088)
2a	343[a]	5560	−6.144 (−6.381)	−2.005 (−2.122)	4.140 (4.260)
6	390[b]	2570	−5.228 (−5.331)	−1.556 (−1.651)	3.672 (3.680)
7a[c]	418	6820	(−5.426)	(−2.086)	(3.340)

[a]Center of broad band with vibration structure of eight narrow peaks (Figure 5). The UV spectrum of **2a** was recorded in this work for the first time. [b]Center of broad band tailing up to 420 nm. [c]Calculations for **7a** were performed for $CHCl_3$ solution only.

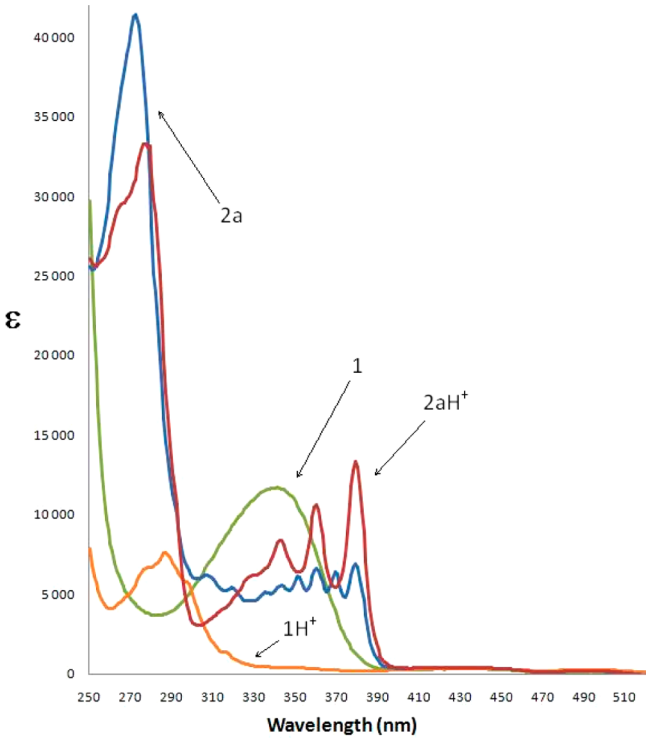

Figure 5. UV−vis spectra of compounds **1**, **2a**, and their protonated forms (in $CHCl_3$).

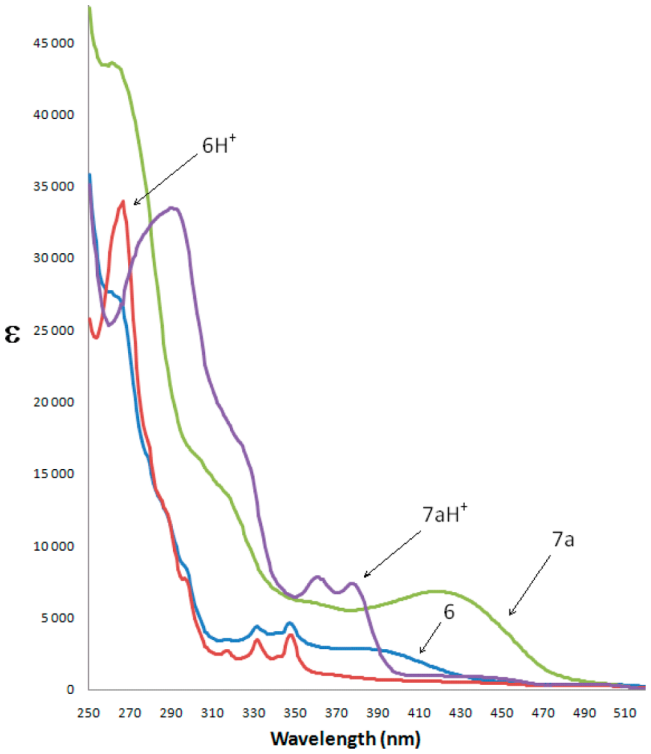

Figure 6. UV−vis spectra of compounds **6**, **7a**. and their protonated forms (in $CHCl_3$).

electrons in the ground state (Figure 8). However, compound **6** in this respect is an exception. Its total vector in the ground state is oriented from the aza toward the 10-NMe_2 group. A simple explanation for this is given in Supporting Information (p S27).

Most impressively the difference in the nature of the excited states of the compounds under consideration is manifested in the electronic spectra of their cations. While in molecule **1** the protonation completely switches off the conjugation (actually the UV spectrum of **1** closely resembles that of naphthalene), in the case of quino[7,8-*h*]quinoline cation **2aH**$^+$ the position and vibrational structure of the long-waved absorption band remain almost unchanged apart from the considerable increase of peak intensity and the reduction in peak number (Figure 5). In their turn, the electronic spectra of cations **6H**$^+$ and **7aH**$^+$ appear as a compromise between the above appearances. Two interaction effects disappear entirely: (a) the conjugation between *peri*-substituents and (b) the conjugation between 10-NMe_2 group and the ring π-system. At the same time, there remains π-interaction with the involvement of naphthalene and heterocyclic rings. Clearly, all these factors are superimposed on one another. Thus, in the UV−vis spectra of cations **6H**$^+$ and **7aH**$^+$ the long wavelength bands undergo hypsochromic shift in comparison with those of the corresponding bases but their end absorption still a bit falls into the visible region (Figure 6). This explains why the protonated salts of **6** and **7** are weakly beige or creamy solids unlike colorless bases **1** and **2a** and yellow-orange bases **6** and **7**.

Fluorescence Properties. We then have examined emission spectra for six representatives of *peri*-NMe_2/—N═ systems and additionally for benzo[*h*]quinoline (**11**). The main spectral parameters including fluorescence lifetimes,τ, of the excited state and a rate constant of radiationless energy loss, k_{nr}, are summarized in Table 5. Usually, toluene was employed as a solvent, but in several cases acetonitrile was also taken. Illustratively, the absorption, excitation, and emission spectra of compounds **6**, **7a**, and **11** are shown in Figure 9 (for spectra of other studied compounds, see Figures S32−S36, Supporting Information).

The data obtained lead to the following conclusions. There is no doubt that the conjugation of *peri*-substituents in **6** and **7** plays the decisive role in their ability to fluoresce in the visible region. Best of all, this is confirmed by disappearance of the fluorescence on transition from bases **6** and **7** to their

DOI: 10.1021/acs.joc.6b00917
J. Org. Chem. 2016, 81, 5574−5587

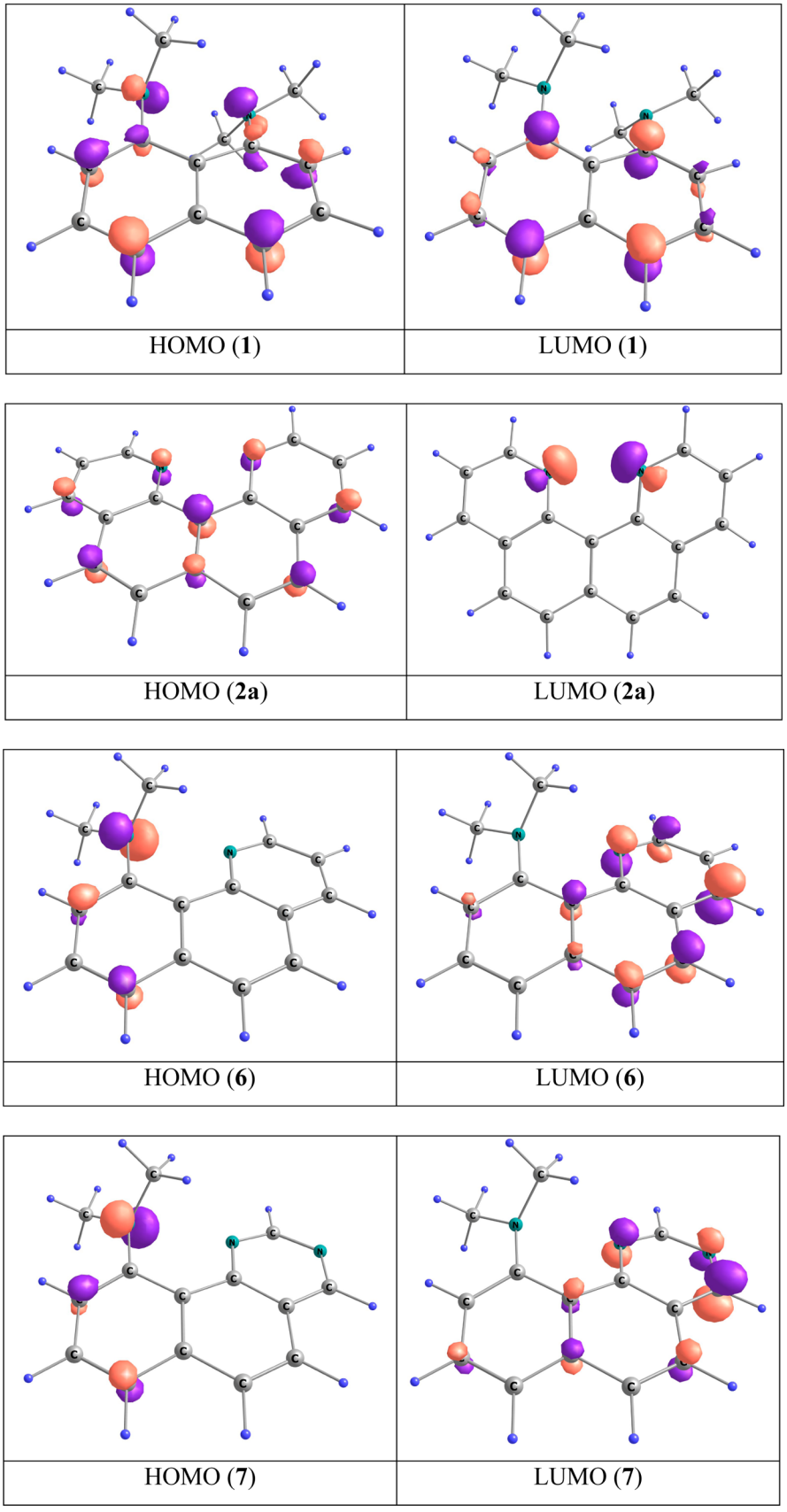

Figure 7. HOMO and LUMO orbitals (B3LYP/6-311++G**, chloroform) for compounds **1**, **2a**, **6**, and 10-dimethylaminobenzo[*h*]quinazoline **7** (R^1 = R^2 = R^3 = H).

DOI: 10.1021/acs.joc.6b00917
J. Org. Chem. 2016, 81, 5574−5587

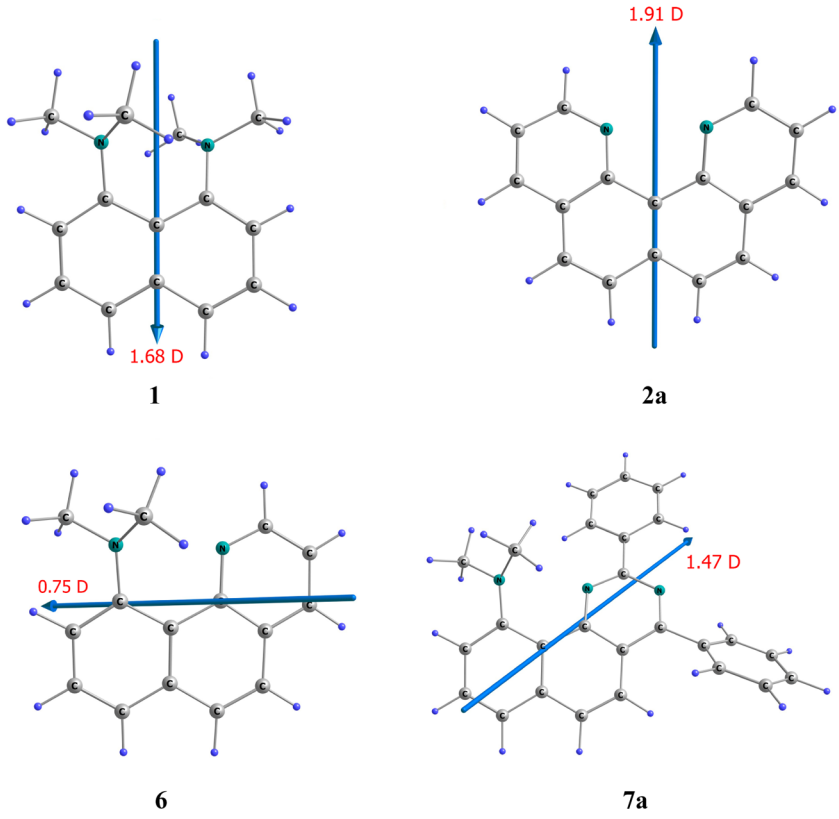

Figure 8. Calculated gas-phase dipole moments and their total vectors in molecules of proton sponge **1** and its mono- (**6**) and diaza- (**2a**, **7a**) analogues (B3LYP/6-311++G**).

Table 5. Selected Absorption and Emission Parameters of the Studied Compounds

compd	solvent	absorption, λ_{max}, nm (ε)	emission, λ_{max}, nm	stokes shift, nm (cm^{-1})	quantum yield, Φ	τ, ns	k_{nr}, $s^{-1} \times 10^{-10}$
4	PhMe	371 (16700)	506	47 (2020)	0.025	1.3	3.0
		429 (7220)					
		459 (6530)					
6	PhMe	349 (3910)	477	89 (4810)	0.016	0.9	6.8
		388 (3710)					
6	MeCN	342 (3480)	500	119 (6250)	0.003	0.4	83
		381 (3730)					
7a	PhMe	421 (6990)	520	99 (4520)	0.015	1.1	6.0
7a	MeCN	416 (6500)	569	153 (6460)	0.001	0.4	249
7b	PhMe	298 (32330)	507	88 (4140)	0.021	1.2	3.9
		419 (8190)					
7c	PhMe	443 (8050)	546	103 (4260)	0.006		
7d	PhMe	298 (17800)	493	93 (4720)	0.021	1.6	2.9
		354 (5650)					
		400 (6530)					
11	PhMe	316 (1370)	349	3 (248)			
		330 (2660)	365				
		338 (1140)	384				
		346 (3290)					
11	MeCN	314 (1220)	350	5 (414)			
		329 (2270)	365				
		337 (1020)	383				
		345 (2660)					

protonated forms (Figure 9d). A weakly pronounced fluorescence of proton sponge **1**[29] and benzo[*h*]quinoline also agrees with this viewpoint. Thus, the electronic absorption spectrum of **11** in toluene exhibits a group of narrow bands at 330, 338, and 360 nm characterizing the $\pi \rightarrow \pi^*$ transitions that are typical for polynuclear aromatic systems (Figure 9b). In the emission spectrum, these bands undergo red shift and appear with λ_{max} = 349, 365, and 389 nm testifying fluorescence of the $\pi\pi^*$ origin from the lowest excited singlet state where the $n\pi^*$ transitions are expected to be higher in energy.[30]

DOI: 10.1021/acs.joc.6b00917
J. Org. Chem. 2016, 81, 5574−5587

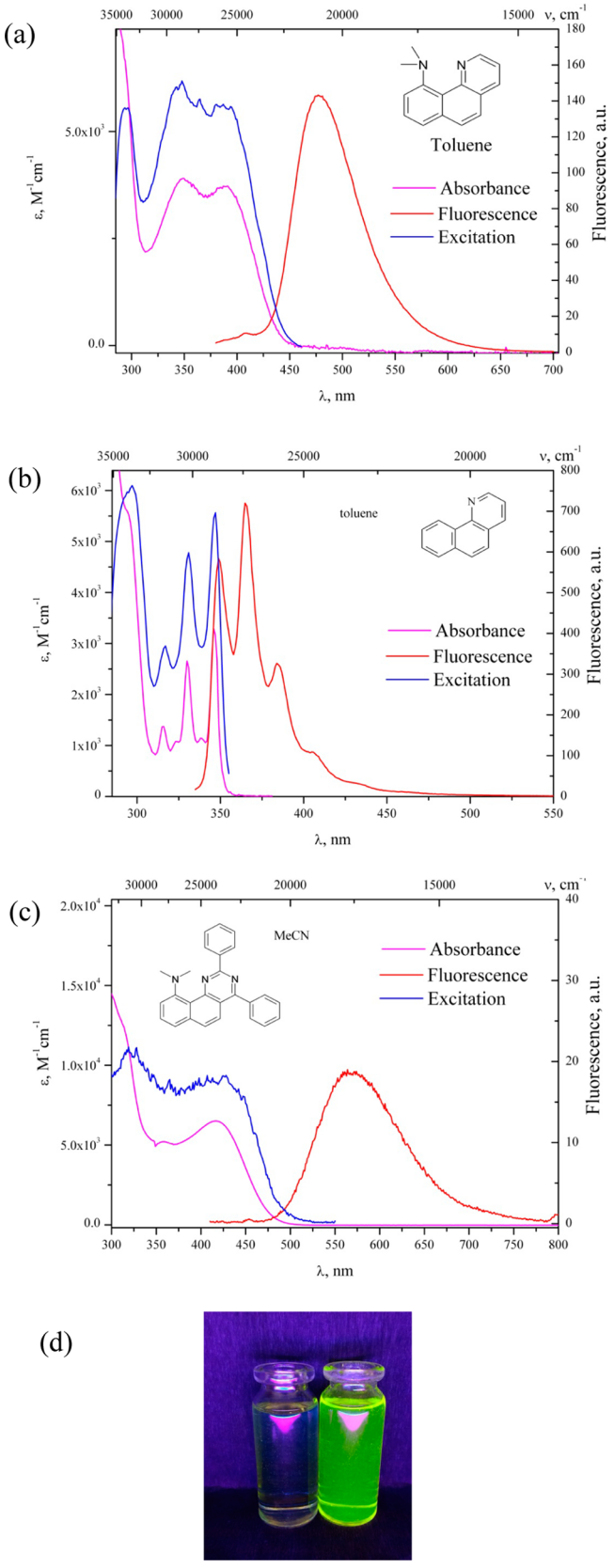

Figure 9. Absorption (purple line), excitation (blue), and emission (red) spectra of 1 × 10^{-5} M solutions: (a) **6a** in toluene, (b) benzo[*h*]quinoline (**11**) in toluene, and (c) **7a** in acetonitrile. (d) Visual portrayal of compound **7a** as base (right vial) and tetrafluoroborate salt **7a**·HBF_4 (left vial) under UV irradiation (1·10^{-3} M chloroform solution).

Increasing solvent polarity upon passing from PhMe to MeCN causes almost no influence on the position of the absorption and emission bands in **11**.

Placing the *peri*-NMe_2 group into the benzo[*h*]quinoline skeleton (compound **6**) results in broadening the long wavelength absorption band and its bathochromic shift of about 40 nm (Figure 9a). The fluorescence spectrum of **6** is characterized by a structureless broad band in the 400−650 nm region centered at 477 nm. Similar but even more pronounced spectral changes occur for compounds **7** (Figure 9c, Figures S33−S36 in Supporting Information).

The Stokes shift values, which compounds **6** and **7** display in toluene, are about 90 nm. However, in acetonitrile solution they increase to 120 nm for **6** and 153 nm for **7a**. Such influence of more polar MeCN indicates that excitation is manifested as $S_o \rightarrow S_{\pi\pi^*}$, not $S_o \rightarrow S_{n\pi^*}$, electronic transition. Larger value of the Stokes shift for **7a** likely results from the more extended π-system in it due to the presence of two phenyl substituents if compared, for example, with **6** and **7d**.[31] Notably, that the Stokes shifts for **6** and **7** are about 1 order of magnitude (in cm^{-1}) higher than that found for **11**.

The quantum yield of fluorescence of the studied compounds is rather low, especially in polar MeCN solutions, varying from 0.001 (**7a**, MeCN) to 0.025 (**4**, toluene). Decreasing the emission intensity and shortening fluorescence lifetime in MeCN can be attributed to a very fast nonradiative relaxation of the emissive ICT state via the twisting of highly mobile NMe_2 groups in *peri*-disubstituted naphthalenes;[13,29] this overpopulates the twisted structure (TICT-state) having weakly emissive character.[32] Finally, it should be mentioned that the transition from **6** and **7a**−**d** to 9-bromoderivative **7e** leads to a much weaker emission (fluorescence quantum yield cannot be reliably determined) that is likely caused by the enhancement of intersystem crossing.

■ CONCLUSIONS

In summary, we have conducted a thorough study of 10-dimethylamino derivatives of benzo[*h*]quinoline **6** and benzo[*h*]quinazolines **7** as typical representatives of almost unknown *peri*-NMe_2/—N═ superbasic systems. It resulted in disclosing both some similarities and substantial differences in their properties relatively those of *peri*-NMe_2/NMe_2 (kinetically inert proton sponges) and —N═/—N═ (kinetically active pseudo-proton sponges) systems. As expected, the compounds studied display rather high basicity and form chelated monoprotonated cations in which the NH proton is magnetically strongly deshielded. Surprisingly, in contrast to the so-called "aniline−pyridine" rule, the chelated proton in $\mathbf{6H}^+$ and $\mathbf{7H}^+$ cations is considerable shifted to the NMe_2, not to the aza group. In some cases, a fast low-barrier movement of the NH proton was observed. Probably, the most remarkable difference between the NMe_2/—N═ compounds and their NMe_2/NMe_2 and —N═/—N═ counterparts consists in coloration and fluorescence of the former resulting from conjugation between two *peri*-substituents. Finally, the structural criterion was suggested in the work allowing assignment of organic superbases to proton sponges or to pseudo-proton sponges.

■ EXPERIMENTAL SECTION

General Methods. CHN analysis was accomplished by combustion analysis (Dumas and Pregl method). Melting points were determined in glass capillaries and are uncorrected. Flash column chromatography was performed on Al_2O_3. ^1H and ^{13}C NMR spectra

DOI: 10.1021/acs.joc.6b00917
J. Org. Chem. 2016, 81, 5574−5587

were recorded on 250 and 600 MHz spectrometers. Chemical shifts are referred to TMS. The quantum yield of fluorescence was determined using quinine sulfate in 0.1 M H_2SO_4–water (Φ = 0.53 ± 0.023)[33] as reference with optically matched samples having absorbances of 0.1 at λ_{ex} = 365 nm; the experimental error in Φ_f is ±20%. The emission lifetimes were measured using a time-correlated single-photon-counting picosecond spectrophotometer. The sample was excited by a 40 ps pulsed laser centered at 371 nm, and the emission signal was collected at the magic angle. The instrument response function (IRF) was recorded under described conditions by replacing the sample with a Ludox solution. The time decay data were analyzed by nonlinear least-squares fitting with deconvolution of the IRF using the FluoFit software package.[34]

X-ray Diffraction Analysis. Crystals suitable for X-ray studies (Mo Kα line, graphite monochromator, $\omega/2\theta$-scanning) were grown by slow evaporation from solutions of compounds in appropriate solvents: **6·HBF$_4$** (ethanol), **7a·HClO$_4$** (slow diffusion of Et_2O into MeCN), **7e·HClO$_4$** (ethanol). The structures were solved by direct method and refined by the full-matrix least-squares against F^2 in anisotropic (for non-hydrogen atoms) approximation. All hydrogen atoms were placed in geometrically calculated positions and were refined in isotropic approximation in riding model with the U_{iso}(H) parameters equal to $nU_{eq}(C_i)$ (n = 1.2 for CH and CH_2 groups and n = 1.5 for CH_3 groups), where $U(C_i)$ are the equivalent thermal parameters of the atoms to which corresponding H atoms are bonded. The H(N) hydrogen atoms were found in the difference Fourier synthesis and were refined isotropically without any constraints. The main crystallographic data and some experimental details are given in Tables 1, 3, and S1 (Supporting Information). CCDC 1473948–1473950 contain the supplementary crystallographic data for this paper. These data can be obtained free of charge from the Cambridge Crystallographic Data Centre via www.ccdc.cam.ac.uk/data_request/cif.

Quantum Chemical Calculations. Calculations were done according to the density functional theory in split-valence basis set 6-311++G** using B3LYP approach.[35−37] Solvation effects were taken into account by Tomasi polarizable continuum model (PCM).[38] HOMO and LUMO were characterized using natural bond orbital (NBO) analysis. Optimization of the geometry of stationary points was carried out to the gradient value of 10^{-7} hartree/bohr by Gaussian 03 software[39] on the Silver cluster at the Department of Chemistry, Southern Federal University. Transition states were located by using quadratic synchronous transit method (QST2).[40,41] The nature of stationary points was identified under the calculation of normal vibration frequencies through the Hessian matrix. The minimum energy pathways were received by the following gradients from the transition states in both the forward and the reverse directions. Steepest descent was carried out by adding and subtracting 0.1 of imaginary frequency mode to the transition state geometry. It was shown previously[42,43] that the method and basis set that were chosen here provide a good convergence between quantum-chemically calculated parameters and experimental data. In particular, these include bond lengths, valence angles, proton affinities (PA), and gas phase basicities (GPB), as well as relative stability of structures. ChemCraft 1.8 was used for visualization.[44]

10-Dimethylaminobenzo[*h*]quinoline (6). 1-Dimethylamino-8-aminonaphthalene[10] (0.43 g, 2.3 mmol) was thoroughly mixed with sodium *m*-nitrobenzenesulfonate (0.24 g, 1.0 mmol), boric acid (0.058 g, 0.96 mmol), $FeSO_4·7H_2O$ (0.05 g, 0.18 mmol), and glycerol (1.0 mL, 13.5 mmol). Then concn H_2SO_4 (0.45 mL, 8.4 mmol) was gradually added to the mixture with stirring (warming-up!) and heated in an open flask for 1 h at 145 °C. After cooling to 50 °C, the mixture was poured into water (15 mL), the flask was washed with acetone (5 mL), and the combined water–acetone phase was basified to pH 12 with several chips of solid KOH. After stirring and grinding, the resulting mixture was evaporated almost to dryness, and the reaction products were extracted with $CHCl_3$ (50 mL, Soxhlet apparatus), concentrated to a minimal volume, and separated chromatographically. The main brownish fraction of average mobility (Al_2O_3/$CHCl_3$, green luminescence under UV-light) gave quinoline **6** (0.03 g, 6%) as a brown-orange oil. Anal. Calcd for $C_{15}H_{14}N_2$: C, 81.05; H, 6.35; N, 12.60. Found: C, 81.29; H, 6.66; N, 12.38. ^{1}H NMR ($CDCl_3$): δ = 2.95 (6H, s, NMe_2), 7.30 (1H, dd, J = 7.7, J = 0.7 Hz), 7.41–7.47 (2H, m), 7.53–7.62 (2H, m), 7.74 (1H, d, J = 8.7 Hz), 8.09 (1H, dd, J = 8.1, J = 1.9 Hz), 9.08 (1H, dd, J = 4.2, J = 1.9 Hz). ^{13}C NMR ($CDCl_3$): δ = 45.5 (NMe_2), 115.7, 120.1, 121.4, 122.8, 125.9, 127.2, 128.0, 129.0, 135.4, 136.9, 147.3, 147.8, 152.4. UV/vis ($CHCl_3$) λ_{max} (lgε): 257 (sh., 4.45), 316 (3.54), 331 (3.64), 347 (3.66), 381 (3.41), end absorption up to 470 nm. UV/vis ($CHCl_3$ + CF_3CO_2H) λ_{max} (lgε): 266 (4.53), 316 (3.43), 331 (3.54), 347 (3.58).

10-(Dimethylammonium)benzo[*h*]quinoline Tetrafluoroborate (6·HBF$_4$). To an orange-brown solution of quinoline **6** (0.015 g, 0.067 mmol) in EtOAc (1 mL), 1 equiv of aqueous 40% HBF_4 (0.012 mL, 0.070 mmol) was added. The resulting salt was immediately precipitated as a beige flocculent solid, which was additionally phased-out on addition of Et_2O (5 mL). The product was decanted and dried in air to give salt **6·HBF$_4$** (0.017 g, 81%) as light-beige crystals with mp 176–178 °C (from EtOH). Anal. Calcd for $C_{15}H_{15}BF_4N_2$: C, 58.10; H, 4.88; N, 9.03. Found: C, 58.29; H, 4.67; N, 9.32. ^{1}H NMR (CD_3CN): δ = 3.36 (6H, d, J = 4.7 Hz, NMe_2), 7.89–8.04 (3H, m), 8.09–8.16 (2H, m), 8.23 (1H, dd, J = 8.1, J = 1.0 Hz), 8.66 (1H, dd, J = 8.3, J = 1.7 Hz), 9.08 (1H, dd, J = 4.7, J = 1.5 Hz), 17.53 (1H, br. s, N–H···N). ^{1}H NMR (DMSO-d_6): δ = 3.43 (6H, d, J = 4.7 Hz, NMe_2), 7.97–8.07 (2H, m), 8.13 (1H, d, J = 8.9 Hz), 8.21 (1H, d, J = 8.9 Hz), 8.32 (1H, br. d, J = 7.6 Hz), 8.44 (1H, br. d, J = 7.8 Hz), 8.78 (1H, dd, J = 8.3, J = 1.7 Hz), 9.12 (1H, dd, J = 4.6, J = 1.7 Hz), 16.80 (1H, br. s, N–H···N). ^{13}C NMR (CD_3CN): δ = 45.5 (NMe_2), 119.0, 121.2, 123.6, 126.8, 127.8, 128.6, 129.6, 130.4, 135.2, 139.2, 143.2, 144.8, 147.1.

2,4-Disubstituted 10-(Dimethylammonium)benzo[*h*]-quinazoline Tetrafluoroborates (7a–d·HBF$_4$) and Perchlorates (7a,e·HClO$_4$). Compounds **7a–d·HBF$_4$** and **7a,e·HClO$_4$** were obtained similarly to **6·HBF$_4$** from compounds **7a–d** (0.1 mmol) in 87–94% yield using either aqueous 40% HBF_4 or 60% $HClO_4$.[11]

7a·HBF$_4$: Yield 0.043 g (93%), beige crystals with mp 276–280 °C (decomp., from EtOH). Anal. Calcd for $C_{26}H_{22}BF_4N_3$: C, 67.41; H, 4.79; N, 9.07. Found: C, 67.60; H, 4.78; N, 9.13. ^{1}H NMR (CD_3CN): δ = 3.58 (6H, d, J = 4.9 Hz), 7.64–7.78 (6H, m), 7.90–8.00 (2H, m), 8.05–8.33 (5H, m), 8.37–8.47 (2H, m), 16.85 (1H, s). ^{1}H NMR (DMSO-d_6): δ = 3.70 (6H, d, J = 4.6 Hz), 7.68–7.79 (6H, m), 7.91–8.00 (2H, m), 8.11–8.32 (3H, m), 8.38–8.49 (3H, m), 8.57 (1H, d, J = 7.8 Hz), 15.91 (1H, s). ^{13}C NMR (63 MHz, CD_3CN) δ = 46.9, 119.2, 121.0, 122.5, 125.6, 129.2, 129.9, 130.0, 130.6, 131.4, 131.8, 132.0, 132.5, 133.0, 137.1, 137.7, 144.1, 151.3, 160.1, 170.4.

7a·HClO$_4$: Yield 0.042 g (87%), beige crystals with mp 275–277 °C (decomp., from EtOH). Anal. Calcd for $C_{26}H_{22}ClN_3O_4$: C, 65.62; H, 4.66; N, 8.83. Found: C, 65.47; H, 4.83; N, 8.67. ^{1}H NMR (CD_3CN): δ = 3.58 (6H, d, J = 5.0 Hz), 7.66–7.78 (6H, m), 7.91–8.00 (2H, m), 8.05–8.33 (5H, m), 8.38–8.48 (2H, m), 16.86 (1H, s).

7b·HBF$_4$: Yield 0.048 g (92%), beige crystals with mp 240–243 °C (decomp., from EtOH). Anal. Calcd for $C_{28}H_{26}BF_4N_3O_2$: C, 64.26; H, 5.01; N, 8.03. Found: C, 64.13; H, 5.09; N, 7.96. ^{1}H NMR (CD_3CN): δ = 3.53 (6H, d, J = 4.8 Hz), 3.90 (3H, s), 3.93 (3H, s), 7.18 (4H, d, J = 8.4 Hz), 7.91 (2H, d, J = 8.9 Hz), 8.02–8.10 (2H, m), 8.14–8.28 (3H, m), 8.31 (2H, d, J = 9.0 Hz), 17.21 (1H, s). ^{1}H NMR (DMSO-d_6): δ = 3.67 (6H, d, J = 4.5 Hz), 3.91 (3H, s), 3.93 (3H, s), 7.27 (4H, d, J = 8.5 Hz), 7.95 (2H, d, J = 8.7 Hz), 8.10–8.25 (3H, m), 8.38 (3H, d, J = 8.9 Hz), 8.52 (1H, d, J = 7.8 Hz), 16.28 (1H, s). ^{13}C NMR (63 MHz, CD_3CN) δ = 46.8, 56.4, 115.3, 115.9, 119.2, 120.3, 122.3, 125.8, 129.2, 129.3, 130.0, 130.9, 131.8, 132.3, 133.5, 137.7, 144.3, 151.3, 159.7, 163.1, 164.0, 169.7.

7c·HBF$_4$: Yield 0.045 g (94%), light-orange crystals with mp 251–253 °C (decomp., from EtOH). Anal. Calcd for $C_{22}H_{18}BF_4N_3S_2$: C, 55.59; H, 3.82; N, 8.84. Found: C, 55.51; H, 3.88; N, 8.79. ^{1}H NMR (CD_3CN): δ = 3.54 (6H, d, J = 2.9 Hz), 7.29–7.40 (2H, m), 7.80 (1H, d, J = 5 Hz), 7.91 (1H, d, J = 5.1 Hz), 8.02–8.16 (4H, m), 8.21 (1H, d, J = 7.8 Hz), 8.26 (1H, d, J = 8.0 Hz), 8.52 (1H, d, J = 9.2 Hz), 16.45 (1H, s). ^{1}H NMR (DMSO-d_6): δ = 3.65 (6H, d, J = 4.3 Hz), 7.35–7.41 (1H, m), 7.42–7.48 (1H, m), 8.00 (1H, d, J = 4.7 Hz), 8.09–8.30 (5H, m), 8.38 (1H, d, J = 7.9 Hz), 8.51 (1H, d, J = 7.9 Hz), 8.57 (1H,

DOI: 10.1021/acs.joc.6b00917
J. Org. Chem. 2016, 81, 5574–5587

d, J = 9.2 Hz), 15.59 (1H, s). ^{13}C NMR (63 MHz, CD_3CN) δ = 47.0, 119.1, 119.3, 122.6, 124.9, 130.0, 130.2, 130.6, 131.8, 131.9, 132.4, 132.8, 134.2, 134.6, 137.8, 141.3, 141.9, 144.0, 151.4, 156.0, 162.3.

7d·HBF$_4$: Yield 0.040 g (91%), beige crystals with mp 253−255 °C (decomp., from EtOH). Anal. Calcd for $C_{24}H_{26}BF_4N_3$: C, 65.03; H, 5.91; N, 9.48. Found: C, 64.98; H, 5.86; N, 9.42. ^{1}H NMR (CD_3CN): δ = 1.78 (9H, s), 3.53 (6H, d, J = 4.9 Hz), 7.66−7.78 (3H, m), 8.07 (1H, t, J = 8.0 Hz), 8.15 (1H, d, J = 9.4 Hz), 8.22 (1H, dd, J = 7.9, J = 1.0 Hz), 8.29 (1H, dd, J = 8.0, J = 1.0 Hz), 8.39−8.47 (2H, m), 8.65 (1H, d, J = 9.4 Hz), 17.29 (1H, s). ^{1}H NMR (DMSO-d_6): δ = 1.75 (9H, s), 3.64 (6H, d, J = 4.7 Hz), 7.66−7.81 (3H, m), 8.15 (1H, t, J = 8.0 Hz), 8.26 (1H, d, J = 9.4 Hz), 8.36−8.46 (3H, m), 8.52 (1H, d, J = 7.8 Hz), 8.70 (1H, d, J = 9.4 Hz), 16.34 (1H, s). ^{13}C NMR (63 MHz, CD_3CN) δ = 30.7, 42.0, 46.8, 120.0, 121.3, 122.5, 125.6, 128.8, 129.2, 130.7, 131.8, 132.1, 133.0, 137.1, 137.4, 144.2, 151.1, 158.8, 179.9.

7e·HClO$_4$: Yield 0.036 g (65%), yellowish crystals with mp 229−231 °C (decomp., from EtOH). Anal. Calcd for $C_{26}H_{21}BrClN_3O_4$: C, 56.28; H, 3.82; N, 7.57. Found: C, 56.34; H, 3.87; N, 7.50. ^{1}H NMR (CD_3CN): δ = 3.76 (6H, d, J = 4.5 Hz), 7.66−7.81 (6H, m), 7.92−8.00 (2H, m), 8.13 (1H, d, J = 9,2 Hz), 8.19 (1H, d, J = 8.8 Hz), 8.25 (2H, dd, J = 8.9, J = 1.7 Hz), 8.38−8.47 (2H, m), 19.16 (1H, s). ^{13}C NMR (63 MHz, CD_3CN) δ = 43.4, 123.3, 121.4, 126.2, 129.2, 129.9, 130.0, 130.8, 131.5, 132.1, 133.1, 133.4, 136.6, 137.1, 137.5, 138.8, 140.4, 150.5, 159.6, 171.4.

■ ASSOCIATED CONTENT

Supporting Information

The Supporting Information is available free of charge on the ACS Publications website at DOI: 10.1021/acs.joc.6b00917.

^{1}H and ^{13}C NMR spectra for all reported compounds, including the dynamic NMR and pK_a measurements, optimized structures and their energies, illustration of the "pyridine−aniline" basicity rule, UV−vis and fluorescence spectra, and table with crystal data and structure refinement for compounds **6·HBF$_4$**, **7a·HClO$_4$** and **7e·HClO$_4$** (PDF)

X-ray crystallographic data for compound **6·HBF$_4$** (CIF)

X-ray crystallographic data of compound **7a·HClO$_4$** (CIF)

X-ray crystallographic data of compound **7e·HClO$_4$** (CIF)

A text file of all computed molecule Cartesian coordinates in.xyz format for convenient visualization- (XYZ)

■ AUTHOR INFORMATION

Corresponding Author

*E-mail: apozharskii@sfedu.ru (A.F.P.).

Notes

The authors declare no competing financial interest.

■ ACKNOWLEDGMENTS

This work was supported by the Russian Foundation for Basic Research (Project No. 14-03-00010). G.S.B. is grateful to the Ministry of Education and Science (Grant No. 4.967.2014/K) for support of VT NMR experiments. We also thank Drs. Anna V. Tkachuk and Oleg N. Burov (Scientific and Educational Laboratory of Resonance Spectroscopy, Department of Natural and High Molecular Compounds Chemistry, Southern Federal University) for NMR measurements. X-ray studies were performed by Dr. Kyrill Y. Suponitsky (A. N. Nesmeyanov Institute of Organoelement Compounds, Moscow).

■ REFERENCES

(1) (a) Pozharskii, A. F.; Ozeryanskii, V. A. in *The Chemistry of Anilines*; Rappoport, Z., Ed.; J. Wiley & Sons: Chichester, 2007; Part 2, Chapter 17, pp 931−1026. (b) Hodgson, P.; Lloyd-Jones, G. C.; Murray, M.; Peakman, T. M.; Woodward, R. L. *Chem. - Eur. J.* **2000**, *6*, 4451−4460. (c) Perrin, C. L.; Ohta, B. K. *J. Mol. Struct.* **2003**, *644*, 1−12. (d) Perrin, C. L.; Ohta, B. K. *J. Am. Chem. Soc.* **2001**, *123*, 6520−6526.

(2) Pozharskii, A. F.; Ozeryanskii, V. A.; Filatova, E. A. *Chem. Heterocycl. Compd.* **2012**, *48*, 200−219.

(3) (a) Zirnstein, M. A.; Staab, H. A. *Angew. Chem., Int. Ed. Engl.* **1987**, *26*, 460−461. (b) Staab, H. A.; Saupe, T. *Angew. Chem., Int. Ed. Engl.* **1988**, *27*, 865−879.

(4) Hibbert, F. *Acc. Chem. Res.* **1984**, *17*, 115−120.

(5) Kanbara, T.; Suzuki, Y.; Yamamoto, T. *Eur. J. Org. Chem.* **2006**, *2006*, 3314−3316.

(6) (a) Wüstefeld, H.-U.; Kaska, W. C.; Schüth, F.; Stucky, G. D.; Bu, X.; Krebs, B. *Angew. Chem., Int. Ed.* **2001**, *40*, 3182−3184. (b) Shaffer, K. J.; McLean, T. M.; Waterland, M. R.; Wenzel, M.; Plieger, P. G. *Inorg. Chim. Acta* **2012**, *380*, 278−283. (c) Shaffer, K. J.; Wenzel, M.; Plieger, P. G. *Polyhedron* **2013**, *52*, 1399−1402.

(7) (a) Yamasaki, T.; Ozaki, N.; Saika, Y.; Ohta, K.; Goboh, K.; Nakamura, F.; Hashimoto, M.; Okeya, S. *Chem. Lett.* **2004**, *33*, 928−929. (b) Londesborough, M. G. S.; Bould, J.; Baše, T.; Hnyk, D.; Bakardjiev, M.; Holub, J.; Cisarova, I.; Kennedy, J. D. *Inorg. Chem.* **2010**, *49*, 4092−4098. (c) Legare, M.-A.; Courtemanche, M.-A.; Fontaine, F.-G. *Chem. Commun.* **2014**, *50*, 11362−11365.

(8) (a) Llamas-Saiz, A. L.; Foces-Foces, C.; Elguero, J.; Molina, P.; Alajarin, M.; Vidal, A. *J. Chem. Soc., Perkin Trans. 2* **1991**, 2033−2040. (b) Laynez, J.; Menendez, M.; Velasco, J. L. S.; Llamas-Saiz, A. L.; Foces-Foces, C.; Elguero, J.; Molina, P.; Alajarin, M.; Vidal, A. *J. Chem. Soc., Perkin Trans. 2* **1993**, 709−713. (c) Povalyakhina, M. A.; Antonov, A. S.; Dyablo, O. V.; Ozeryanskii, V. A.; Pozharskii, A. F. *J. Org. Chem.* **2011**, *76*, 7157−7166. (d) Belding, L.; Stoyanov, P.; Dudding, T. *J. Org. Chem.* **2016**, *81*, 6−13.

(9) Barić, D.; Dragičević, I.; Kovačević, B. *Tetrahedron* **2014**, *70*, 8571−8576.

(10) Pozharskii, A. F.; Suslov, A. N.; Starshikov, N. M.; Popova, L. L.; Klyuev, N. A.; Adanin, V. A. *Zh. Org. Khim.* **1980**, *16*, 2216−2228; *Chem. Abstr.* **1981**, *94*, 120385s.

(11) Mikshiev, V. Y.; Antonov, A. S.; Pozharskii, A. F. *Org. Lett.* **2016**, *18*, 2872−2875.

(12) Wozniak, K.; Krygowski, T. M.; Kariuki, B.; Jones, W.; Grech, E. *J. Mol. Struct.* **1990**, *240*, 111−118.

(13) (a) Pozharskii, A. F.; Ryabtsova, O. V.; Ozeryanskii, V. A.; Degtyarev, A. V.; Kazheva, O. N.; Alexandrov, G. G.; Dyachenko, O. A. *J. Org. Chem.* **2003**, *68*, 10109−10122. (b) Pozharskii, A. F.; Degtyarev, A. V.; Ryabtsova, O. V.; Ozeryanskii, V. A.; Starikova, Z. A.; Kletskii, M. E.; Sobczyk, L.; Filarowski, A. *J. Org. Chem.* **2007**, *72*, 3006−3019.

(14) (a) Pozharskii, A. F.; Ozeryanskii, V. A. *Russ. Chem. Bull.* **1998**, *47*, 66−73. (b) Klimkiewicz, J.; Koprowski, M.; Stefaniak, L.; Grech, E.; Webb, G. A. *J. Mol. Struct.* **1997**, *403*, 163−165. (c) Klimkiewicz, J.; Stefaniak, L.; Grech, E.; Webb, G. A. *J. Mol. Struct.* **1997**, *412*, 47−50. (d) Grech, E.; Klimkiewicz, J.; Nowicka-Scheibe, J.; Pietrzak, M.; Schilf, W.; Pozharski, A. F.; Ozeryanskii, V. A.; Bolvig, S.; Abildgaard, J.; Hansen, P. E. *J. Mol. Struct.* **2002**, *615*, 121−140.

(15) Toppet, S.; Platteborze, K.; Zeegers-Huyskens, T. *J. Chem. Soc., Perkin Trans. 2* **1995**, 831−834.

(16) The prevailing role of basicity in the location of the NH proton is especially manifested in cation **3H$^+$**.[8b] In the solid **3·HBr**, the NH proton is more shifted to the iminophosphorane group whose nitrogen basicity in Ph−N=PPh$_3$ (pK_a = 8.4, H_2O) exceeds by 4 log that of 1-dimethylaminonaphthalene.

(17) Fringuelli, F.; Marino, G.; Taticchi, A. *J. Chem. Soc. B* **1971**, 2302−2303.

(18) This changing of δ_{NH} value for **4H$^+$** on lowering the temperature independently proves that the pronounced high field shift for the chelated proton signal of ^{1}H NMR of cations **6H$^+$** and

DOI: 10.1021/acs.joc.6b00917
J. Org. Chem. 2016, 81, 5574−5587

$7H^+$ at least partially results from the enhanced asymmetry of their IHBs.

(19) Pozharskii, A. F.; Soldatenkov, A. T.; Katritzky, A. R. *Heterocycles in Life and Society*; J. Wiley: Chichester, U.K., 2011; p 65.

(20) *Comprehensive Heterocyclic Chemistry II*; Katritzky, A. R., Ed.; Pergamon: Oxford, U.K., 1996; Vol. *6*, p 104.

(21) To date, three general types of strong neutral organic bases are distinguished: (1) conventional (kinetically active), (2) proton sponges (lowered kinetic activity), and (3) proton traps ("proton prisons"), usually the caged structures capturing a proton in the inner cavity so tightly that it cannot be removed by ordinary methods.[2] If the border between bases of the two first types and proton traps looks clear, the separation of conventional bases and proton sponges is rather diffuse. Indeed, there are plenty of examples in the literature when bidentate bases such as 2,2′-bipyridine or *o*-phenanthroline are attributed to proton sponges despite their high kinetic activity.[23] Until now, two approaches were put forward to solve this problem. One, proposed by Hibbert,[4] is based on directly measuring the rates of protonation−deprotonation. The second, which is more qualitative, has been mentioned above and provides the ^{1}H NMR study of a mixture of a base and its protonated form (Figure S21, Supporting Information). In the present article, we actually offer a third criterion, which can be termed as structural.

(22) Masuda, Y.; Mori, Y.; Sakurai, K. *J. Phys. Chem. A* **2013**, *117*, 10576−10587.

(23) (a) Elliott, M. C.; Williams, E.; Howard, S. T. *J. Chem. Soc., Perkin Trans. 2* **2002**, 201−203. (b) Mandal, T. K.; Pati, S. K.; Datta, A. *J. Phys. Chem. A* **2009**, *113*, 8147−8151. (c) Vitske, V.; König, C.; Hűbner, O.; Kaifer, E.; Himmel, H.-J. *Eur. J. Inorg. Chem.* **2010**, *2010*, 115−126. (d) Villaverde, G.; Arnanz, A.; Iglesias, M.; Monge, A.; Sanchez, F.; Snejko, N. *Dalton Trans.* **2011**, *40*, 9589−9600. (e) Shaffer, K. J.; Parr, D. C.; Wenzel, M.; Rowlands, G. J.; Plieger, P. G. *Eur. J. Org. Chem.* **2012**, *2012*, 6967−6975. (f) Belding, L.; Dudding, T. *Chem. - Eur. J.* **2014**, *20*, 1032−1037.

(24) Pyzalska, D.; Pyzalski, R.; Borowiak, T. *J. Crystallogr. Spectrosc. Res.* **1983**, *13*, 211−220.

(25) Darabantu, M.; Lequeux, T.; Pommelet, J.-C.; Ple, N.; Turck, A.; Toupet, L. *Tetrahedron Lett.* **2000**, *41*, 6763−6767.

(26) Churakov, A. V.; Shihilov, O. N. *CSD Communication*, CCDC GOKXAH: Experimental Crystal Structure Determination, 2010, DOI: 10.5517/ccvy2jc.

(27) Shang, R. L.; Du, L.; Sun, B.-W. *Acta Crystallogr., Sect. E: Struct. Rep. Online* **2006**, *E62*, o2920−o2921.

(28) *Uspekhi Stereokhimii*; Klyain, V.; de la Mare, P. B. D., Eds.; GNTI Khimicheskoi Literatury: Moscow, 1961; p 547. English ed.: Wepster, B. M. In *Progress in Stereochemistry*; Klyne, W.; de la Mare, P. B. D., Eds.; Butterworths: London, 1954−1958; Vols. *1* and *2*.

(29) Szemik-Hojniak, A.; Zwier, J. M.; Buma, W. J.; Bursi, R.; van der Waals, J. H. *J. Am. Chem. Soc.* **1998**, *120*, 4840−4844.

(30) Harthcock, C.; Zhang, J.; Kong, A. *J. Phys. Chem. A* **2015**, *119*, 11997−12004.

(31) Krasovitskii, B. M.; Bolotin, B. M. *Organic Luminescent Materials*; VCH: New York, 1988; 340 pp.

(32) Ghosh, R.; Palit, D. K. *J. Phys. Chem. A* **2015**, *119*, 11128−11137.

(33) Adams, M. J.; Highfield, J. G.; Kirkbright, G. F. *Anal. Chem.* **1977**, *49*, 1850−1852.

(34) Enderlein, J.; Erdmann, R. *Opt. Commun.* **1997**, *134*, 371−378.

(35) Becke, A. D. *Phys. Rev. A: At., Mol., Opt. Phys.* **1988**, *38*, 3098−3100.

(36) Becke, A. D. *J. Chem. Phys.* **1993**, *98*, 5648−5652.

(37) Lee, C.; Yang, W.; Parr, R. G. *Phys. Rev. B: Condens. Matter Mater. Phys.* **1988**, *37*, 785−789.

(38) Tomasi, J.; Mennucci, B.; Cammi, R. *Chem. Rev.* **2005**, *105*, 2999−3093.

(39) Frisch, M. J.; Trucks, G. W.; Schlegel, H. B.; Scuseria, G. E.; Robb, M. A.; Cheeseman, J. R.; Montgomery, J. A., Jr.; Vreven, T.; Kudin, K. N.; Burant, J. C.; Millam, J. M.; Iyengar, S. S.; Tomasi, J.; Barone, V.; Mennucci, B.; Cossi, M.; Scalmani, G.; Rega, N.; Petersson, G. A.; Nakatsuji, H.; Hada, M.; Ehara, M.; Toyota, K.; Fukuda, R.; Hasegawa, J.; Ishida, M.; Nakajima, T.; Honda, Y.; Kitao, O.; Nakai, H.; Klene, M.; Li, X.; Knox, J. E.; Hratchian, H. P.; Cross, J. B.; Bakken, V.; Adamo, C.; Jaramillo, J.; Gomperts, R.; Stratmann, R. E.; Yazyev, O.; Austin, A. J.; Cammi, R.; Pomelli, C.; Ochterski, J. W.; Ayala, P. Y.; Morokuma, K.; Voth, G. A.; Salvador, P.; Dannenberg, J. J.; Zakrzewski, V. G.; Dapprich, S.; Daniels, A. D.; Strain, M. C.; Farkas, O.; Malick, D. K.; Rabuck, A. D.; Raghavachari, K.; Foresman, J. B.; Ortiz, J. V.; Cui, Q.; Baboul, A. G.; Clifford, S.; Cioslowski, J.; Stefanov, B. B.; Liu, G.; Liashenko, A.; Piskorz, P.; Komaromi, I.; Martin, R. L.; Fox, D. J.; Keith, T.; Al-Laham, M. A.; Peng, C. Y.; Nanayakkara, A.; Challacombe, M.; Gill, P. M. W.; Johnson, B.; Chen, W.; Wong, M. W.; Gonzalez, C.; Pople, J. A. *Gaussian 03*, revision D.01; Gaussian, Inc.: Wallingford, CT, 2003.

(40) Halgren, T. A.; Lipscomb, W. N. *Chem. Phys. Lett.* **1977**, *49*, 225−232.

(41) Peng, C.; Schlegel, H. B. *Isr. J. Chem.* **1993**, *33*, 449−454.

(42) Dyablo, O. V.; Pozharskii, A. F.; Shmoilova, E. A.; Ozeryanskii, V. A.; Fedik, N. S.; Suponitsky, K. Yu. *J. Mol. Struct.* **2016**, *1107*, 305−315.

(43) Moser, A.; Range, V.; York, D. M. *J. Phys. Chem. B* **2010**, *114*, 13911−13921.

(44) Zhurko, G. A.; Zhurko, D. A. Chemcraft, http://www.chemcraftprog.com.

DOI: 10.1021/acs.joc.6b00917
J. Org. Chem. 2016, 81, 5574−5587